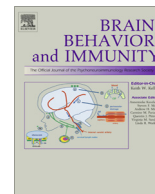




Contents lists available at ScienceDirect

Brain, Behavior, and Immunity

journal homepage: www.elsevier.com/locate/ybrbi

The neuron-specific interleukin-1 receptor accessory protein is required for homeostatic sleep and sleep responses to influenza viral challenge in mice

Christopher J. Davis^{a,*}, Danielle Dunbrasky^a, Marcella Oonk^a, Ping Taishi^a, Mark R. Opp^b, James M. Krueger^a

^a College of Medical Sciences and the Sleep and Performance Research Center, Washington State University Spokane, Spokane, WA 99210, United States

^b Department of Anesthesiology & Pain Medicine, University of Washington, Seattle, WA 98104, United States

ARTICLE INFO

Article history:

Received 24 July 2014

Received in revised form 14 October 2014

Accepted 23 October 2014

Available online xxxx

Keywords:

Cytokine

H1N1

Recuperation

PR8

Sleep deprivation

Mouse

ABSTRACT

Interleukin-1 β (IL1) is involved in sleep regulation and sleep responses induced by influenza virus. The IL1 receptor accessory protein (AcP) and an alternatively spliced isoform of AcP found primarily in neurons, AcPb, form part of the IL1 signaling complex. IL1-induced sleep responses depend on injection time. In rat cortex, both IL1 mRNA and AcPb mRNA peak at Zeitgeber Time (ZT) 0 then decline over the daylight hours. Sleep deprivation enhances cortical IL1 mRNA and AcPb mRNA levels, but not AcP mRNA. We used wild type (WT) and AcPb knockout (KO) mice and performed sleep deprivation between ZT10 and 20 or between ZT22 and 8 based on the time of day expression profiles of AcPb and IL1. We hypothesized that the magnitude of the responses to sleep loss would be strain- and time of day-dependent. In WT mice, NREMS and REMS rebounds occurred regardless of when they were deprived of sleep. In contrast, when AcPbKO mice were sleep deprived from ZT10 to 20 NREMS and REMS rebounds were absent. The AcPbKO mice expressed sleep rebound if sleep loss occurred from ZT22 to 8 although the NREMS responses were not as robust as those that occurred in WT mice. We also challenged mice with intranasal H1N1 influenza virus. WT mice exhibited the expected enhanced sleep responses. In contrast, the AcPbKO mice had less sleep after influenza challenge compared to their own baseline values and compared to WT mice. Body temperature and locomotor activity responses after viral challenge were lower and mortality was higher in AcPbKO than in WT mice. We conclude that neuron-specific AcPb plays a critical role in host defenses and sleep homeostasis.

Published by Elsevier Inc.

1. Introduction

Interleukin-1 β (IL1) is part of the molecular sleep homeostat in health and disease (Krueger, 2008; Imeri and Opp, 2009). Injection of exogenous IL1 enhances non-rapid eye movement sleep (NREMS) in multiple species. At low somnogenic doses IL1 has little effect on rapid eye movement sleep (REMS) or body temperature. Higher doses can inhibit both NREMS and REMS and induce fever (Opp et al., 1991). Inhibition of IL1 using anti-IL1 antibodies, or a soluble IL1 receptor, or the IL1 receptor antagonist reduces the time spent in NREMS (reviewed Krueger, 2008). Further, mice lacking the type I IL1 receptor have less spontaneous NREMS and REMS during the night hours. These mice also lack the ability to generate

sleep responses to exogenous IL1 (Fang et al., 1998). Brain levels of IL1 mRNA vary with the time of day with highest levels occurring at Zeitgeber Time (ZT) 0, the beginning of the sleep period (Taishi et al., 1997, 2012). Inhibiting caspase-1, the enzyme cleaves the pro-form of IL1 to produce mature IL1, reduces spontaneous NREMS and attenuates sleep responses to lipopolysaccharide (LPS; Imeri et al., 2006). Lastly, after sleep loss and infectious challenge, sleep and brain levels of IL1 mRNA or IL1 protein are enhanced (Taishi et al., 1998; Leyva-Grado et al., 2009; reviewed Imeri and Opp, 2009).

The IL1 receptor accessory protein (IL1R AcP) binds to the IL1/IL1 receptor complex triggering a biochemical signaling cascade. An alternatively-spliced isoform of the IL1R AcP, the neuron-specific IL1R AcP, called AcPb, is expressed predominately in brain (Smith et al., 2009; Huang et al., 2011; Taishi et al., 2012). Previously we showed that in response to sleep loss, AcPb mRNA, but not AcP mRNA, is up-regulated in brain (Taishi et al.,

* Corresponding author at: P.O. Box 1495, Spokane, WA 99202, United States. Tel.: +1 509 358 7820.

E-mail address: cjdavis@wsu.edu (C.J. Davis).

1998, 2012). Maximum spontaneous levels of brain AcPb mRNA occur at ZT0, as do IL1 mRNA levels. Further, exogenous somnogenic doses of IL1 enhance brain AcPb mRNA, but not AcP mRNA. These results collectively suggest the involvement of AcPb in spontaneous sleep regulation and in the expression of sleep responses induced by sleep loss or microbial challenge.

Influenza A/PR/8/34 (PR8) is an H1N1 human strain adapted to replicate in mice. PR8 is found in the brain olfactory bulb (OB) within 4 h post-intranasal instillation (PI) (Majde et al., 2007). Pro-inflammatory cytokine mRNAs, including IL1, are elevated in the OB at 15 h PI when the mice become overtly ill when a high dose of virus is used (Majde et al., 2007). Virus appears to be restricted to glia of the outer layers of the OB, but the number of IL1-expressing neurons increases in olfactory and autonomic pathways with projections from the olfactory system (Leyva-Grado et al., 2009). Illness onset correlates with increased numbers of IL1-expressing neurons in the hypothalamus, a sleep regulatory area (Leyva-Grado et al., 2009).

In this study, we determined the sleep responses of wild type (WT) mice and mice lacking the AcPb (AcPb knockout [KO]) mice to sleep deprivation and in separate experiments sleep and sickness responses to influenza virus challenge. We report that AcPbKO mice have attenuated sleep responses after sleep loss and virus challenge.

2. Materials and methods

2.1. Animals

Male C57BL/6 mice (control strain) were from Jackson Laboratories, (Bar Harbor, ME) and male IL1 receptor AcPb knockout (KO) mice (experimental strain), were provided by Amgen (Seattle, WA) and bred for 5–7 generations at Washington State University, were used in these studies. Subsequent homozygote offspring were used in the experiments. Mice were sleep deprived or infected at 2–3 months of age. Breeding mice were maintained on a 14:10 h light–dark cycle and experimental mice were on a 12:12 light–dark cycle (light onset = ZT0). All mice were genotyped from tail snips by Transnetyx (Cordova, TN). Mice were maintained in plastic filter-top cages at 23–24 °C and during recordings in sound-attenuated environmental chambers. Food and water were available *ad libitum*. All animal procedures were approved by the Washington State University Animal Care and Use Committee and conformed to National Institutes of Health guidelines.

Mice used for polysomnographic analyses were anesthetized with an intraperitoneal (ip) injection of ketamine–xylazine (87 and 13 mg/kg, respectively) for surgical implantation of electroencephalographic (EEG) electrodes over the right and left parietal cortices and over the cerebellum, which acted as a ground as previously described (Taishi et al., 2012). In addition, a stainless steel electromyogram (EMG) electrode was placed in the dorsal neck muscles. The electrodes were fixed on the head with dental cement. Mice were allowed at least 7 days to recover from the surgical procedure and to acclimate to the tethered polysomnographic cables. In an independent experiment, biotelemetry transmitters (Minimitter, Bend, OR) were chemically sterilized and implanted intraperitoneally via the anesthesia regimen reported above. Mice were allowed to recover for at least 1 week after surgery and housed individually in cages placed atop ER-4000 receiver plates.

2.2. Polysomnographic recording and analyses

Polysomnographic recording cables connected the head electrodes to commutators that were in turn led to amplifiers. The analog EEG and EMG signals from the amplifiers were converted to

digital signals (128 Hz sampling rate) and recorded. EEG signals were filtered below 0.1 Hz and above 100 Hz with a 60 Hz notch filter. EEG analyses were conducted using Sleep Sign Software (Kissei Comtec Co., Ltd., Japan). Vigilance states including wakefulness, NREMS, and rapid-eye movement sleep (REMS) were manually determined off-line in 10 s epochs as described previously (Taishi et al., 2012). Briefly, NREMS was characterized by high-amplitude EEG signals and low EMG activity. REMS was identified by regular low-amplitude EEG and minimal EMG activity. Wakefulness was determined when the signal exhibited low amplitude fast EEG and high EMG activity. Time spent in REMS or NREMS, the duration and frequency of REMS or NREMS episodes were calculated in 2 h or 12 h time blocks. After artifact exclusion from individual NREMS-scored epochs, EEG signals were analyzed by fast Fourier transformation using a Hanning window. NREMS EEG slow wave activity (SWA; 0.5–4 Hz) was determined within each epoch. The means of the 24 h EEG SWA control values for each mouse were used as a reference value to normalize the data for both the control and experimental treatment days as previously described (Krueger et al., 2010). EEG SWA values for each animal were determined for 2 h or 12 h time bins and presented as a percentage of the 24 h baseline values. In addition, power spectra in the 0–20 Hz range were extracted for the first 4 h post-SD or the 12 h light or dark period. These data were normalized using a 24 h average of the NREMS-scored 0–20 Hz spectral content comprised of 1 Hz bin sums from 2 h or 12 h periods of individual mice.

2.2.1. Sleep deprivation and recovery

2.2.1.1. Experiment 1a: SD ZT22–8. Age-matched mice ($n = 8/\text{strain}$) were placed in sound attenuated recording chambers and acclimated to the headstage and cables for 2 days prior to recording a 24 h baseline ZT8–8. Then mice were subjected to gentle handling SD for a 10 h period from ZT22 to 8 as previously described (Taishi et al., 2012). The 10 h SD periods in Experiments 1a and 1b were selected based on the sleep deficits in IL1 type I receptor KO mice which occur from ZT12 to 20 (Fang et al., 1998) and the differences in the timing of IL1 and AcPb cortical gene expressions (Taishi et al., 2012). EEG recordings continued for 24 h after the end of SD to document the recovery sleep/wake responses. Two mice were excluded due to the loss of headcap interface and one due to the detection of seizure activity during manual scoring. Thus, six WT mice and seven AcPbKO mice were used in subsequent sleep analyses.

2.2.1.2. Experiment 1b: SD ZT10–20. Mice ($n = 12/\text{strain}$) were acclimated and baseline recorded as above, except that the 24 h baseline was recorded from ZT20 to 20. In this study, gentle-handling SD occurred from ZT10 to 20. EEG recordings ensued for 24 h after SD. Whereas, the previous ZT22–8 SD study was completed in two rounds, this study used a third round to confirm by replication the absence of rebound sleep to ZT10–20 SD, reported hereafter. Two WT mice were excluded from the study due to the loss of a headcap interface. Accordingly, data from ten WT and 12 AcPbKO mice were analyzed.

2.2.1.3. Virus purification and titration. A mouse-adapted H1N1 A/Puerto Rico/8/34 H1N1 (PR8) influenza virus (lot # 3X010621) was suspended in pyrogen-free allantoic fluid (Specific Pathogen-Free Avian Supply, North Franklin, CT) and purified by ultracentrifugation sucrose-gradient sedimentation as previously described (Grimm et al., 2007; Majde et al., 2007). The virus was diluted to a protein concentration of 200 µg/ml, aliquoted, frozen on dry ice, and stored at –80 °C. A standard hemagglutination assay with twofold dilutions of purified PR8 (10 µl) mixed with 50 µl chicken red blood cells and incubated at room temperature for 30 min yielded 1×10^7 virus particles/ml. Samples were tested

for endotoxin using a Limulus lysate gel-clot assay (Biowhittaker, Walkersville, MD); endotoxin was below detection levels. Additionally, the purified virus was negative for mycoplasma and acholeplasma contamination as determined by nested PCR. In Madin-Darby canine kidney cells (MDCK; ATCC, Manassas, VA), viral titrations were assessed and expressed as median tissue culture infectious doses (TCID₅₀) as described elsewhere (Grimm et al., 2007). The starting titer of purified PR8 virus was 2.5×10^4 TCID₅₀/ml.

2.2.1.4. Body temperature and locomotor activity recording and analyses. Telemetric signals were recorded at 6 min intervals, and data points derived from those values were averaged over 6 h bins for body temperature and activity. Activity counts for every 6 h and from each mouse were normalized by dividing the 6 h value by its total 24 h activity count and are expressed as a percent of baseline. Baseline was recorded for 24 h beginning at ZT0 and continued for 9 days. Morbidity was visually determined by daily examination of online temperature graphs and the criteria established for euthanasia were mice showing $<31^\circ\text{C}$ for 12 h.

2.2.2. Influenza virus challenge

2.2.2.1. Experiment 2a: PR8 infection and polysomnography. WT ($n = 13$) or AcPbKO ($n = 7$) mice were acclimated to the experimental chambers and instrumentation for 2 days before recording a 24 h baseline ZT0–0. Then each mouse received 12.5 TCID₅₀ of purified mouse-adapted PR8 influenza virus. The live virus delivery occurred by intranasal instillation of 50 μL of purified PR8, 25 μL per nostril, under 20% isoflurane/80% polyethylene glycol (isoflurane-PEG) anesthesia. The intranasal virus was given within 1 h of light onset (ZT0–1). After viral challenge, mice were placed back in their recording chambers and EEG and EMG were recorded for the next 8 days. Three AcPbKO mice were omitted due to loss of headcap, so 13 WT mice and 7 AcPbKO mice were included for data analyses. Data attrition on PI Day 4 was due to a failed UPS battery backup for the recording system. Attrition on subsequent recording days occurred when an animal died or was euthanized after succumbing to the infection.

2.2.2.2. Experiment 2b: PR8 infection, body temperature and locomotor activity. WT ($n = 11$) or AcPbKO ($n = 11$) mice were acclimated to the recording chamber for at least 1 week after surgery before recording a 24 h baseline for temperature and activity. Next, mice were infected using the same technique and dose as above, returned to their cages and recordings ensued for the next 9 days.

2.2.2.3. Statistical analyses. In Experiments 1a and 1b, mixed three-way ANOVAs, performed in SPSS v17.0, were used to assess factors of strain (WT vs. AcPbKO), treatment (baseline vs. post-SD), and time (in 2 h bins) for the dependent variables: time spent in NREMS or REMS, number of bouts and bout lengths of REMS and NREMS, in addition to NREMS EEG SWA. A three-way mixed ANOVA was used to compare NREMS spectral power with repeated measures of spectral frequency (0–20 Hz), treatment, and strain as an independent factor. A Huynh–Feldt adjustment was used to mitigate sphericity violations of the repeated measures, however the unadjusted degrees of freedom are reported for clarity. In Experiment 2a, two-way ANOVAs (strain and treatment) were run on light and dark periods separately using differences from baseline values for each of the response variables reported above, except for the power spectra analyses which were performed as above. *A priori* comparisons of baseline vs. post PI days were performed when a significant treatment effect was detected on the raw or normalized values, not difference scores. Temperature and activity data were analyzed with a mixed three-way ANOVA in 6 h bins in Experiment 2b. Post hoc comparisons were made using independent or paired *t*-tests when appropriate. In Experiment 2b

the alpha level of the *t*-tests was adjusted to $p < 0.01$ to account for additional comparisons incurred with 6 h bins over 10 days, for all other analyses $p < 0.05$ was considered statistically significant.

3. Results

3.1. Sleep deprivation and recovery

3.1.1. Experiment 1a: SD ZT22–8

After 10 h of SD from ZT22 to 8, WT mice showed the expected NREMS rebound after SD [Treatment \times Time: $F_{(11,121)} = 5.62$, $p < 0.001$]. The rebound was evident in the remaining 4 h light period immediately after SD (ZT8–12) within which WT mice had an additional 22 min of NREMS over their baseline values (Fig. 1A). The AcPbKO mice had 12 min of extra NREMS during the initial 4 h after SD, but this increase was not significant (Fig. 1A). The NREMS rebound continued during the subsequent dark period (ZT12–0) in both strains with 50 min extra NREMS in WT mice [*t*-test, $p < .05$] and 57 min additional NREMS in AcPbKO mice [*t*-test, $p < .001$], each compared with their respective baseline values (data not shown). Compared to baseline the average duration of NREMS epochs increased during ZT8–12 after SD [Treatment \times Time: $F_{(11,121)} = 2.96$, $p < 0.01$] by an average of 62 s in WT mice and 78 s in AcPbKO mice (Fig. 1D), whereas the number of NREMS epochs decreased [Treatment \times Time: $F_{(11,121)} = 6.98$, $p < 0.001$; data not shown] by an average of 6.5 in WT and 12.5 in AcPbKO mice. The differences between strains with either NREMS epoch duration or frequency were not significant.

REMS in WT mice roughly doubled in the first 4 h post-SD (ZT8–12) with respect to baseline levels [Treatment \times Time: $F_{(11,121)} = 8.34$, $p < 0.001$], with a cumulative increase of 13 min (Fig. 1B). Compared to WT mice, the REMS rebound in AcPbKO mice was significantly attenuated with 9 min of extra REMS above their baseline values during ZT8–12 (Fig. 1B). The REMS rebound continued in both strains into the following dark period (ZT12–0) [Strain \times Time: $F_{(11,121)} = 1.90$, $p < 0.05$; data not shown] with 11 min increase from baseline in WT mice [*t*-test, $p < 0.01$] and 12 min in AcPbKO mice [*t*-test, $p < 0.01$]. During ZT8–12, the 4 h immediately after SD, the average REMS epoch length increased compared to baseline [Treatment \times Time: $F_{(11,121)} = 2.85$, $p < 0.01$] by an average of 30 s in WT mice and 16 s in AcPbKO mice (Fig. 1E), and the number of REMS epochs also increased [Treatment \times Time: $F_{(11,121)} = 4.19$, $p < 0.001$; data not shown] by an average of 2.5 in WT and 1.0 in AcPbKO mice. The strain differences for REMS epoch duration and frequency were significant [Strain \times Treatment: $F_{(11,121)} = 2.23$, $p < 0.05$, and $F_{(11,121)} = 2.37$, $p < 0.05$, respectively]. Further, there was a significant REMS epoch length decrease for AcPbKO mice during ZT8–10 as compared with WT mice.

During the initial 4 h after SD (ZT8–12), WT and AcPbKO mice (Fig. 1C) displayed the typical NREMS EEG SWA increase with respect to their respective baseline records [Treatment \times Time: $F_{(11,99)} = 9.04$, $p < 0.001$]. In the subsequent dark period following SD (ZT12–0), both strains demonstrated a negative rebound as occurs in mice after SD and is characterized by delayed decrease in NREMS EEG SWA (data not shown). Spectral content of the NREMS EEG from the ZT8 to 12 periods was altered by SD [Treatment \times Hz: $F_{(19,171)} = 33.06$, $p < 0.001$]. In WT mice, the increases in the 1–3 Hz band and decreases in the 5–6 and 6–7 Hz bands (Fig. 1F). In AcPbKO mice, SD enhanced power in the 1–3 and 9–10 Hz ranges (Fig. 1F). No significant differences between strains occurred for either NREMS EEG SWA or the power spectrum.

3.1.2. Experiment 1b: SD ZT10–20

WT mice subjected to SD from ZT10 to 20 had excess NREMS during the immediate subsequent 4 h, ZT20–24 (Fig. 2A). In

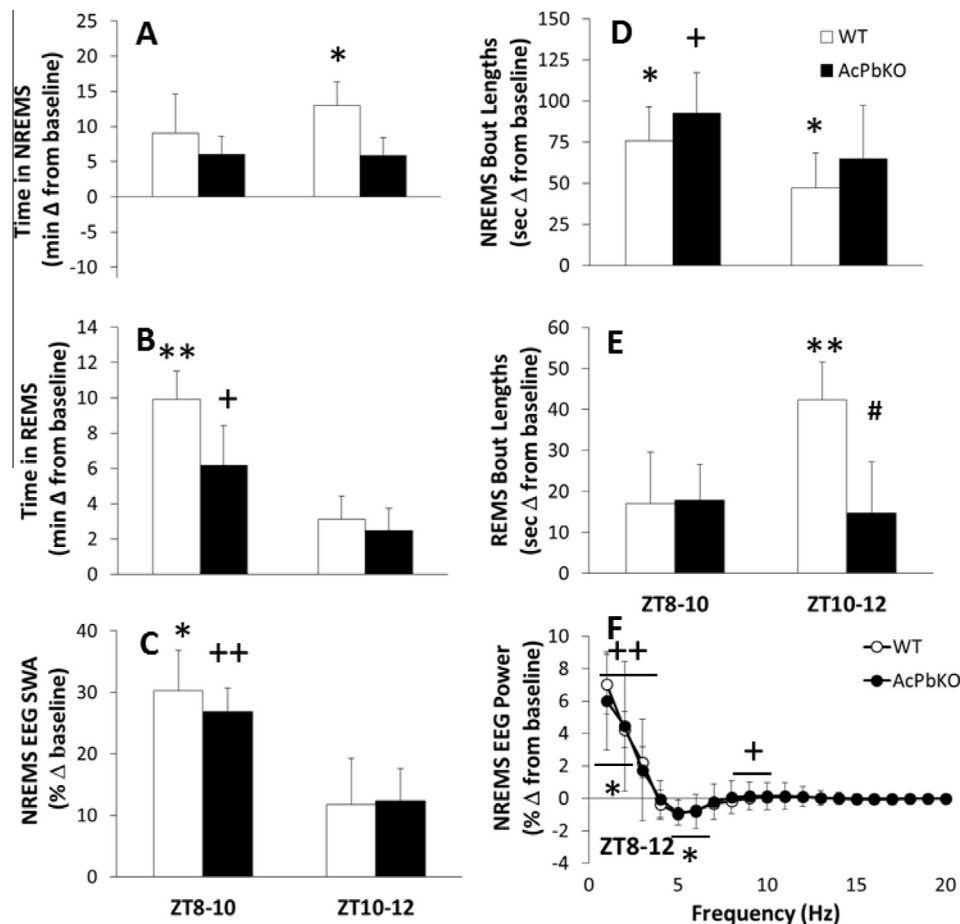


Fig. 1. AcPbKO mice have attenuated sleep responses to sleep loss. WT and AcPbKO mice were deprived of sleep from ZT22 to 8 and then allowed to spontaneously sleep the next day. NREMS, REMS, NREMS EEG SWA and spectral responses for the first 4 h post-sleep deprivation (ZT8–12) are shown as difference from baseline; during this period sleep rebound responses are maximum (* $p < 0.05$, ** $p < 0.01$, WT baseline vs. SD; + $p < 0.05$, ++ $p < 0.01$, AcPbKO baseline vs. SD; # $p < 0.05$ WT vs. AcPbKO).

contrast, AcPbKO mice failed to produce a NREMS rebound in response to SD from ZT10 to 20 (Fig. 2A); in fact they had 6 min less NREMS than their baseline values in the first 4 h after SD [Strain \times Treatment \times Time: $F_{(11,220)} = 1.34$, $p < 0.05$]. There was a significant difference in NREMS duration during ZT20–22 between strains (Fig. 2A). In either strain, there were no NREMS increases during the subsequent post-SD light period (ZT0–12; data not shown). In the first 4 h after SD, NREMS epoch lengths increased by 20 s in WT mice and 25.5 s in AcPbKO mice [Treatment \times Time: $F_{(11,220)} = 2.36$, $p < 0.05$], but only the values obtained during the first 2 h post-SD in WT were significant (Fig. 2D). The number of NREMS epochs during ZT20–0 did not change in WT mice, and was reduced by 7.5 in AcPbKO mice [Treatment: $F_{(1,20)} = 6.23$, $p < 0.05$]. During the post-SD light period NREMS epoch lengths did not differ from respective baseline values. Moreover, no significant strain differences in NREMS epoch length or frequency were observed at any time block.

After SD from ZT10 to 20, REMS rebound occurred within the initial 4 h post-SD (ZT20–24) in WT mice [significant during ZT20–22; Fig. 2B, Treatment \times Time: $F_{(11,220)} = 2.29$, $p < 0.05$], whereas no significant rebound occurred in AcPbKO mice (Fig. 2B). Further, the REMS rebound in WT mice persisted (data not shown), and was significant at ZT2–4, 10–12 and 12–14. Despite the reported treatment differences occurring within the strains, there were no significant strain effects in REMS durations. REMS epoch lengths increased [Strain \times Treatment \times Time: $F_{(11,220)} = 1.94$, $p < 0.05$] by 17.5 s in WT mice (significant between ZT20 and 22; Fig. 2E) and 4.5 s in AcPbKO mice (significant

between ZT22 and 0; Fig. 2E) in the 4 h immediately after SD (ZT20–24), but did not differ from baseline in the subsequent light period (ZT0–12; data not shown). Finally, SD also increased REMS epoch frequency in WT mice but not in AcPbKO mice [Strain \times Treatment \times Time: $F_{(11,220)} = 1.94$, $p < 0.05$; data not shown].

Between ZT20 and 0, the 4 h dark period right after SD, NREMS EEG SWA was greater than baseline values in WT and AcPbKO mice [Fig. 2C; Treatment \times Time: $F_{(11,198)} = 13.18$, $p < 0.001$]. In both strains these effects were significant during the first 2 h (ZT20–22). Further, in AcPbKO mice a compensatory decrease in NREMS EEG SWA occurred during ZT10–12 (data not shown). During the 4 h post-SD periods, spectral content changed in both strains [Treatment \times Hz: $F_{(19,342)} = 11.66$, $p < 0.001$]. In WT mice, power increased in the 1–20 Hz range (Fig. 2F), whereas in AcPbKO mice, increases occurred in the 1–4 and 12–15 Hz bands after SD (Fig. 2F). No statistically significant strain differences were found for either NREMS EEG SWA or the power spectrum.

3.2. Influenza virus challenge

3.2.1. Experiment 2a: sleep responses to PR8 infection

The dose of influenza virus used in the current experiments was lower than the dose of the same virus preparation used in our prior work to allow a slower onset of morbidity and mortality; thus the effects of the virus on sleep took longer to manifest. Consistent with the literature, NREMS amounts in the dark increased following infection in WT mice [Fig. 3A, Day: $F_{(3,40)} = 2.94$, $p < 0.05$]. For

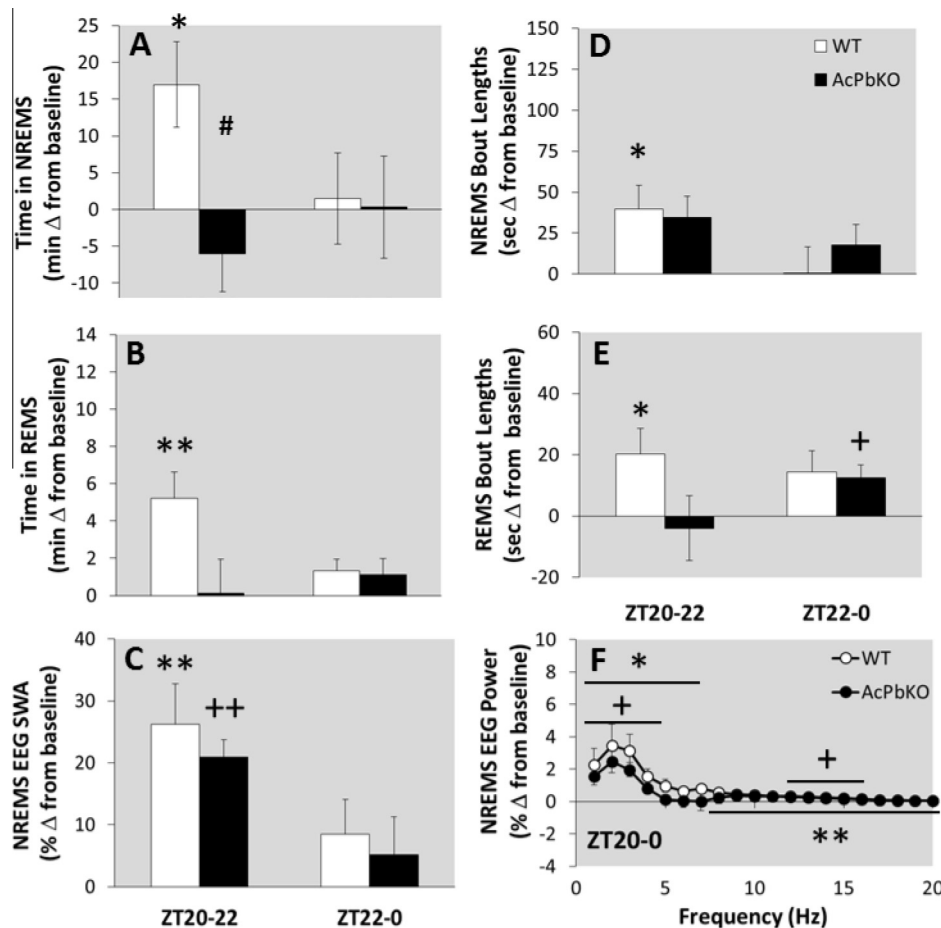


Fig. 2. AcPbKO mice lack NREMS rebound and REMS rebound is reduced compared to WT mice after sleep deprivation from ZT10 to ZT20. WT and AcPbKO mice were deprived of sleep from ZT10 to ZT20 then allowed to spontaneously sleep for the 24 h. NREMS, REMS, NREMS EEG SWA and spectral responses for the first 4 h post-sleep deprivation (ZT20–0) are shown as difference from baseline (* $p < 0.05$, ** $p < 0.01$, WT baseline vs. SD; * $p < 0.05$, ** $p < 0.01$, AcPbKO baseline vs. SD; # $p < 0.05$ WT vs. AcPbKO; shaded background indicates lights off).

instance, on PI Day 8, WT mice had more NREMS during the 12 h dark period (ZT12–0) compared to their own baseline values [t -test, $p < 0.01$]. In contrast, the AcPbKO mice had less NREMS in the ZT12–0 period after viral challenge compared to WT mice [Fig. 3C, Strain: $F_{(1,59)} = 7.66$, $p < 0.01$] on PI Day 8 [t -test; $p < 0.05$], but the PI AcPbKO NREMS values were not different from the AcPbKO baseline values. Time in NREMS did not differ in either strain during the light period. After infection, there were significant changes between strains in the number and length of NREMS bouts that occurred during the light [Fig. 3B and D, Strain: $F_{(1,59)} = 12.58$, $p < 0.01$; bout length not shown, Strain: $F_{(1,59)} = 17.58$, $p < 0.01$, respectively] and dark periods [Fig. 3B and D; Strain: $F_{(1,59)} = 30.25$, $p < 0.001$; bout length not shown, Strain: $F_{(1,59)} = 7.28$, $p < 0.01$, respectively]. Although time in NREMS was not different during the light in either strain, on PI day 6, WT mice averaged 155.67 more NREMS bouts [t -test; $p < 0.05$] with 31.8 s shorter bout duration [t -test, $p < 0.01$] compared to AcPbKO mice, indicating that NREMS sleep was more fragmented in WT mice. This effect was even more apparent during the dark phase, when WT mice spent more time in NREMS. On PI day 6, WT mice had 256.8 more NREMS bouts [t -test, $p < 0.01$] with 17.5 s less bout length [t -test, $p < 0.001$] and on PI day 8 they had 155.2 more NREMS bouts [t -test, $p < 0.01$] with a 16.4 s decrease in bout length [t -test, $p < 0.001$] with respect to AcPbKO mice. While several statistically significant treatment changes were detected using t -tests on single PI days, non-significant factorial analyses disallowed

such comparisons. Thus, treatment effects for light or dark periods are not reported for NREMS bout counts or bout lengths.

Time spent in REMS decreased in WT mice during the light and dark periods as compared with their baseline amounts [Fig. 3E, Day: $F_{(3,40)} = 9.51$, $p < 0.001$; Day: $F_{(3,40)} = 2.83$, $p = 0.05$, respectively]. On PI day 6, WT mice had 17.3 min less REMS during the light [t -test, $p < 0.05$] and 6.1 min less REMS during the dark period [t -test, $p < 0.01$]. Attenuated REMS in WT mice continued on PI day 8 with a 40.9 min reduction from baseline [t -test, $p < 0.001$] during the light period and a 8.7 min decrease in REMS during the dark [t -test, $p < 0.01$]. In AcPbKO mice treatment differences in REMS amounts were not detected during the light period, however REMS decreases from baseline were present in the dark period [Fig. 3G, Day: $F_{(3,38)} = 3.30$, $p < 0.05$] with –10.2 min [t -test, $p < 0.01$] and –11.01 min [t -test, $p < 0.01$] on PI days 6 and 8, respectively. The suppressed REMS during the light period in WT mice following viral challenge was absent in AcPbKO mice [Strain: $F_{(1,59)} = 24.62$, $p < 0.001$] and significantly different on PI days 6 [t -test, $p < 0.05$] and 8 [t -test, $p < 0.01$]. During the dark period strain differences in REMS amounts were not statistically significant. The number of REMS bouts in WT mice decreased from baseline during the light and dark periods [Fig. 3F, Day: $F_{(3,40)} = 10.12$, $p < 0.001$; Day: $F_{(3,40)} = 5.88$, $p = 0.01$, respectively] on the PI days 6 [t -test, $p < 0.05$] and 8 [t -test, $p < 0.01$] during the light and PI day 8 during the dark [t -test, $p < 0.01$]. In AcPbKO mice REMS bout frequency was elevated from baseline during the light, but not dark, periods

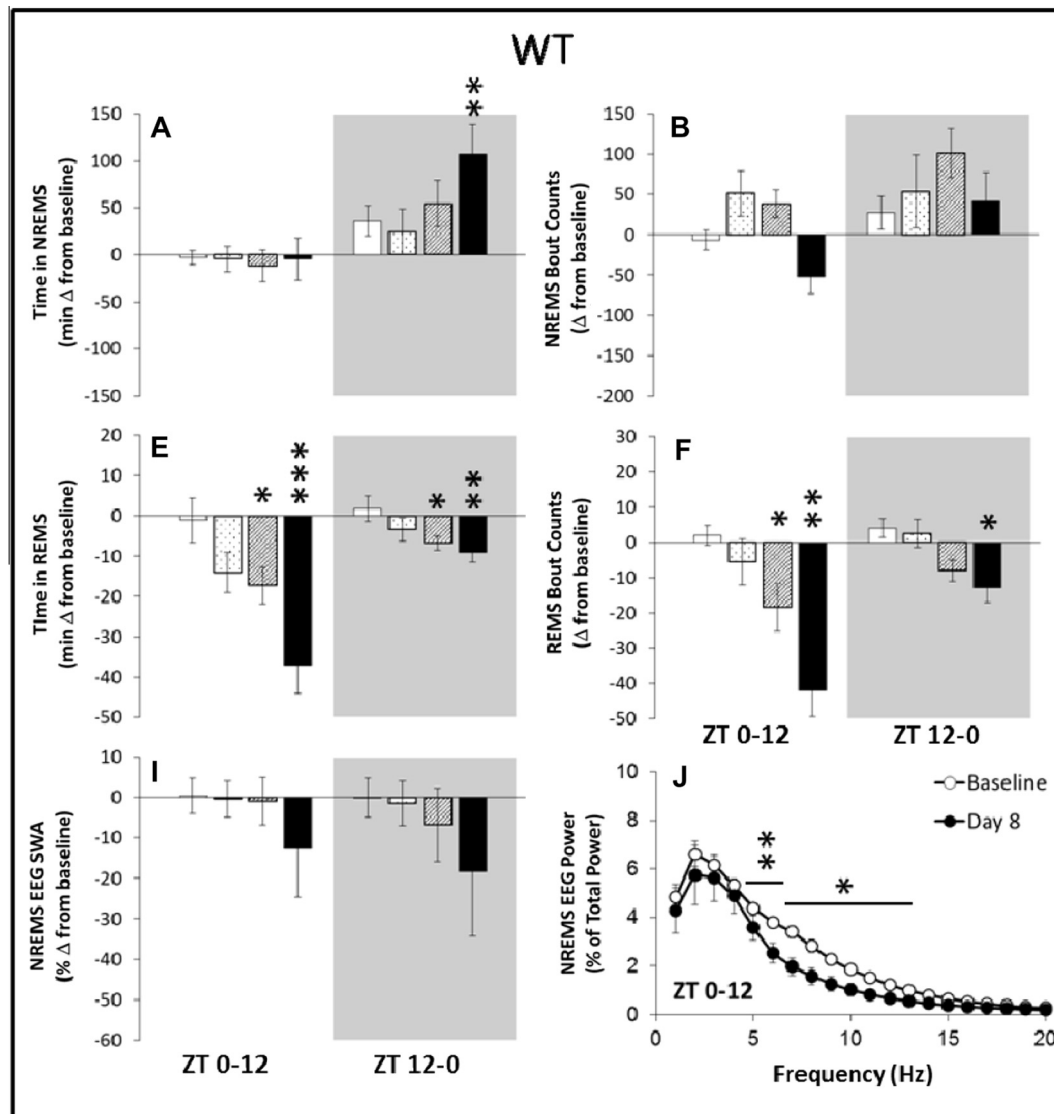


Fig. 3. AcPbKO mice have blunted sleep responses to influenza virus challenge. The AcPbKO mice had less NREMS during nighttime hours (shaded areas representing the 12 h dark period) than their corresponding baseline values. In contrast, WT mice increased NREMS during this period. REMS was inhibited on Day 8 post-viral challenge in WT mice, but not AcPbKO mice. The AcPbKO mice also had lower EEG SWA values during NREMS (* $p < 0.05$, ** $p < 0.01$, WT baseline vs. post injection day; * $p < 0.05$, ** $p < 0.01$, AcPbKO baseline vs. post injection day and * $p < 0.05$, ** $p < 0.01$, WT vs. AcPbKO).

(Fig. 3H) and strain differences were detected via a significant interaction effect [Strain \times Day: $F_{(3,59)} = 4.11$, $p < 0.05$]. REMS bout lengths were not different from baseline on any specific day in either strain. However during the light period, WT mice had 29.2 [t -test, $p < 0.05$] and 58.8 [t -test, $p < 0.001$] fewer REMS bouts than AcPbKO mice on PI day 6 and 8, respectively. WT mice also had longer REMS bouts, than AcPbKO mice [not shown, Strain: $F_{(1,59)} = 18.69$, $p < 0.001$] on PI day 6 by 29.2 s [t -test, $p < 0.05$; on PI day 8, t -test $p = 0.05$]. Despite the increased bout durations in the dark, the decreased REMS amounts coupled with fewer REMS bouts during the light and dark periods in WT mice, is consistent with the literature and indicate an atypical REMS response to viral challenge in AcPbKO mice.

Compared to WT mice (Fig. 3I), AcPbKO mice (Fig. 3K) had larger reductions of NREMS EEG SWA in the light and dark periods following viral challenge [Strain: $F_{(1,54)} = 12.97$, $p < 0.001$; Strain: $F_{(1,54)} = 4.14$, $p < 0.05$, respectively], but the changes were only significant on PI day 6 [t -tests, $p < 0.05$ for light and dark periods] because both strains had their largest decreases on PI day 8. Although NREMS EEG SWA was significant different from baseline

on specific PI days in AcPbKO, but not in WT mice, main effects of Day were not present in light or dark periods and therefore excluded.

In WT mice, EEG FFT spectral content in the higher frequency ranges was also affected [Fig. 3J; Day: $F_{(4,70)} = 3.61$, $p < 0.05$] on PI Day 8; decreases in the 6–13 Hz and 6–16 Hz ranges for the light and dark periods, respectively. In AcPbKO mice on PI Day 8, reductions in EEG FFT power occurred in the 1–4 Hz and 6–7 Hz ranges during the light [Fig. 3L, Day: $F_{(4,70)} = 3.31$, $p < 0.05$], but the decreases during the dark period were not statistically significant (not shown).

3.2.2. Experiment 2b: temperature and activity responses to PR8 infection

The onset of hypothermia [Fig. 4A, Strain \times Day: $F_{(9,180)} = 4.97$, $p < 0.05$] and locomotor activity deficits [Fig. 4B, Strain \times Day: $F_{(9,180)} = 2.85$, $p < 0.05$] following infection were more severe in AcPbKO mice and were accompanied with higher mortality rates (Fig. 4C). The strain differences for both sickness measures were apparent on PI day 3 and continued to varying degrees through

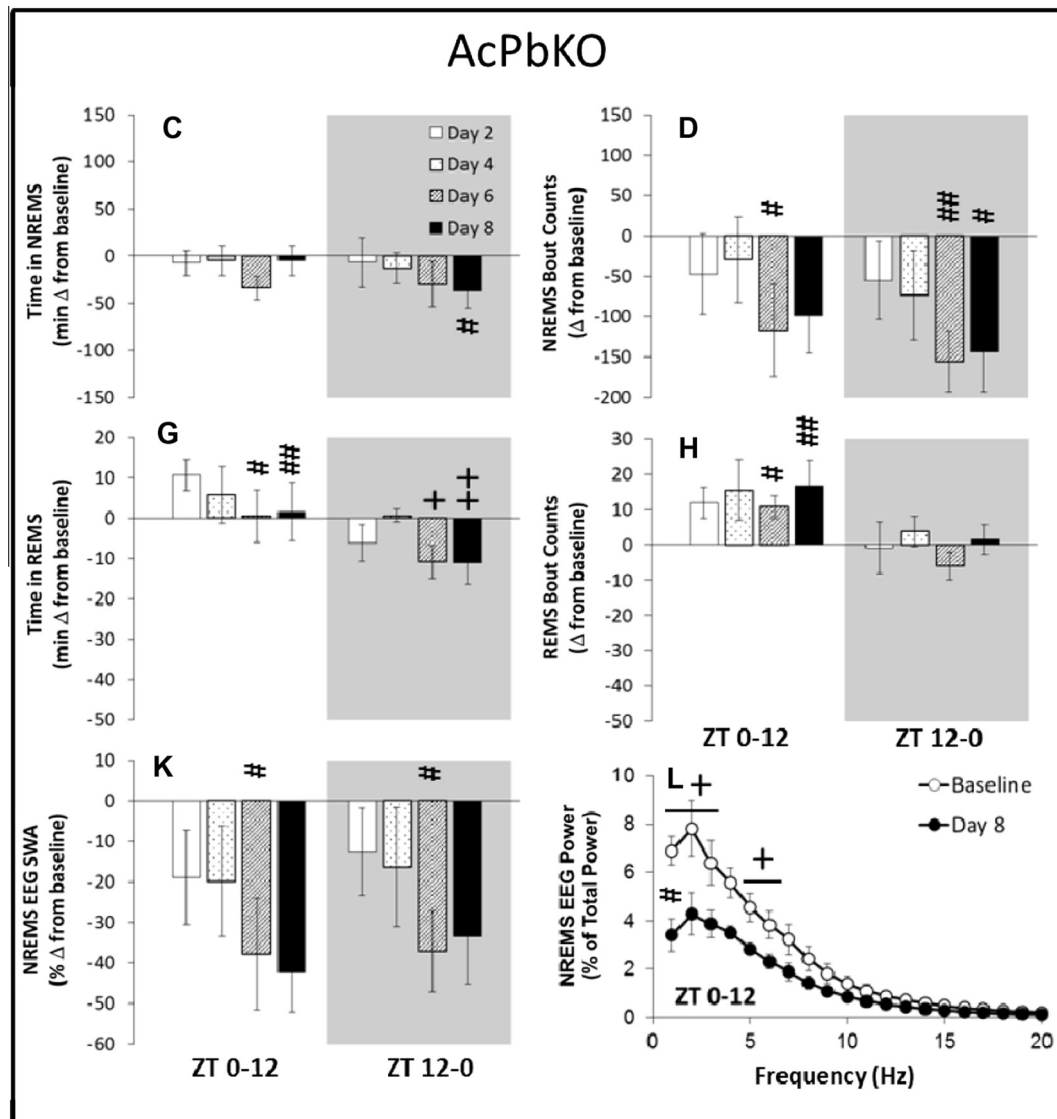


Fig. 3 (continued)

PI day 9. For instance, on PI Day 8, WT mice showed a 2.02 °C reduction in temperature [Day: $F_{(1,10)} = 12.86$, $p < 0.01$] and a corresponding 58% decrement in activity [Day: $F_{(1,10)} = 23.14$, $p < 0.01$] from baseline. Comparatively, in AcPbKO mice, more dramatic decreases from baseline temperature [-3.96 °C; $F_{(1,10)} = 71.63$, $p < 0.001$] and activity [-80% ; $F_{(1,10)} = 15.82$, $p < 0.001$] occurred on PI Day 8.

4. Discussion

The AcPbKO mouse responses to SD indicate a substantive role for AcPb in sleep homeostasis regulation (Figs. 1 and 2). Of particular interest is that NREMS rebound is absent in AcPbKO mice, but not in WT mice, following ZT10–20 SD. Although not statistically significant during the first 2 h after SD ($p = 0.06$), AcPbKO mice sleep less than their own baseline control values after SD (Fig. 2A) and lack a rebound in the 20 h thereafter as indicated by cumulatively summing of NREMS differences from baseline in the post-SD hours (e.g. ZT20–0, ZT20–4, etc.) never yields a positive number. Further, the loss of NREMS rebound is not substituted by REMS as the post-SD REMS increase is negligible (Fig. 2B), nor is it compensated by higher sleep intensity in AcPbKO mice as evi-

denced by NREMS EEG SWA levels comparable to the levels observed in WT mice (Fig. 2C). We conclude that AcPb plays a role in sleep homeostasis to the extent that it is required for sleep rebound after SD during ZT10–20.

The effects of SD between ZT10 and 20 are distinct from those following SD from ZT22 to 8 in their magnitude, timing and in AcPb mice the direction of effects on NREMS. Prior work suggests multiple interactions with IL1 signaling and the circadian clock. Thus, in rats injection of IL1 during the dark enhances NREMS while the same dose given during light hours reduces NREMS (Opp et al., 1991). SD has different effects on recovery sleep that are dependent upon when the sleep loss occurs in both rats (Tobler and Borbely, 1986; Vyazovskiy et al., 2007) and mice (Huber et al., 2000; Franken et al., 2001). Mice lacking the type I IL1 receptor have less spontaneous sleep during the night than WT mice, but not during the day (Fang et al., 1998). IL1 β and its receptors fluctuate across the day (Taishi et al., 1997, 1998, 2012). Further, both IL1 and AcPb mRNAs are up-regulated by SD (Taishi et al., 1998, 2012). Peak somatosensory AcPb mRNA and IL1 mRNA expressions occur at ZT0 although during the preceding dark hours, ZT12–0, the IL1 mRNA relative values decrease proportionately less than AcPb mRNA values whereas for the hours ZT0–8 AcPb values are less

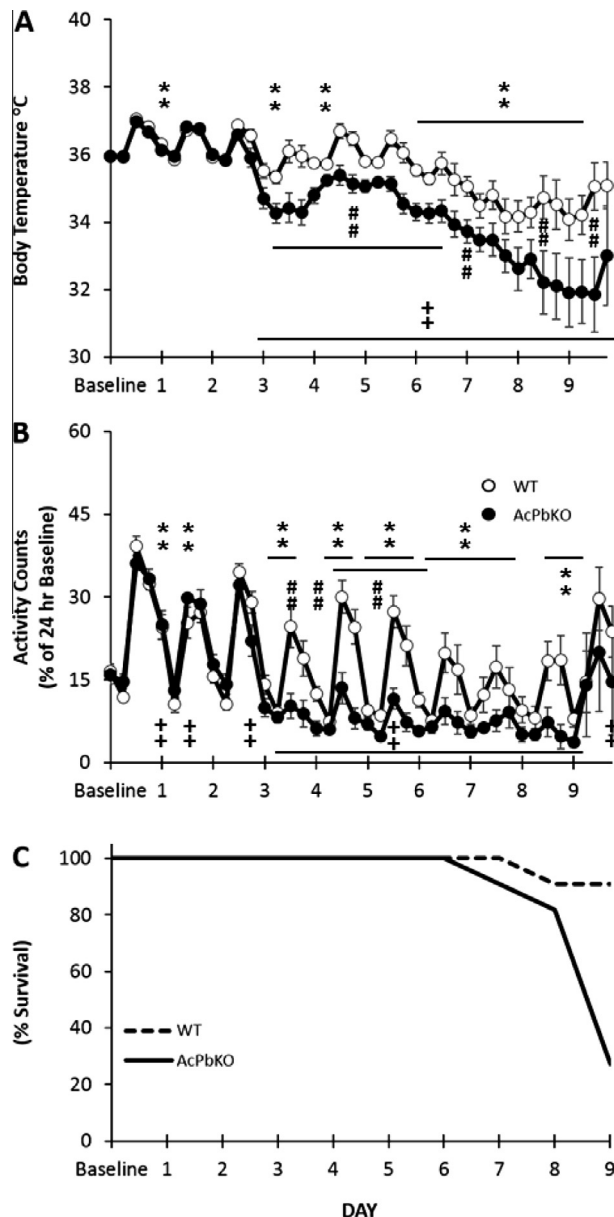


Fig. 4. AcPbKO mice are more hypothermic, less active and have higher mortality than WT mice following viral challenge. Decreased temperature and activity symptoms present on post-infection Day 3 in AcPbKO mice and post-infection Day 6 in WT mice (** $p < 0.01$, WT baseline vs. post injection day; ** $p < 0.01$, AcPbKO baseline vs. post injection day; ## $p < 0.01$ WT vs. AcPbKO).

than IL1 values (Taishi et al., 2012). Further, IL1 inhibits the expression of period 1, 2 and 3 via Clock-Bmal1-induced activation of E-box regulatory elements (Cavadini et al., 2007). Collectively such findings suggest IL1 signaling mechanisms interacting with circadian rhythm mechanisms manifest uniquely at different times of the day to affect sleep; current results are consistent with this conclusion.

There is a robust literature linking sleep and sleep loss to host defenses (reviewed Toth and Jhaveri, 2003; Imeri and Opp, 2009; Zielinski and Krueger, 2011; Besedovsky et al., 2012). Indeed, chronic sleep loss is associated with chronic inflammation; sleep loss-induced up-regulation of IL1 and other cytokines are involved in these inflammatory processes. A separate literature describes the relationships between infectious challenge, and the associated severe inflammation, and other inflammatory stimuli such as LPS and sleep responses as a component of host defenses (reviewed

Majde and Krueger, 2005). Current results suggest that AcPb is also a key component in sleep responses to inflammation to the extent that AcPbKO mice slept less following viral challenge and ultimately this correlated with higher morbidity and mortality. This finding is consistent with earlier work in rabbits showing a correlation between robust sleep responses to infectious challenge and lower morbidity (Toth et al., 1993). Similar findings were reported in bacteria-infected *drosophila* that had less sleep rebound after sleep deprivation also had increased mortality rates (Kuo and Williams, 2014). These data directly support the link between sleep and innate immunity and overall health as shown here and in other reports (Toth and Jhaveri, 2003; Imeri and Opp, 2009; Zielinski and Krueger, 2011; Besedovsky et al., 2012).

Severe influenza infection in mice is characterized by a precipitous reduction in body temperature (Wong et al., 1997) together with a disappearance of circadian temperature rhythms (Conn et al., 1995; Majde et al., 2007). This is consistent with our sleep EEG and temperature patterns in WT mice (Figs. 3A, E and 4A). Similar NREMS increases restricted to the dark phase following infection in WT mice were reported by Toth and Verhulst (2003). The AcPbKO mice maintain their sleep rhythms as observed by REMS and NREMS amounts after viral challenge, yet their temperature rhythms deteriorated earlier and to a greater extent than in WT mice (Fig. 4A). Infected mice demonstrate reduced locomotor activity that is also accompanied by a loss of circadian rhythms (Conn et al., 1995) this was apparent in AcPbKO mice on Day 3 several days before the reductions occurred in WT mice (Fig. 4B). The time of onset and severity of these responses to mouse-adapted influenza virus in a particular mouse strain is determined by the dose of virus administered (Conn et al., 1995; Toth et al., 1995; Fang et al., 1995). Herein, we infected with a lower dose than used previously in our lab (e.g. Majde et al., 2007, 2010; Leyva-Grado et al., 2009) and accordingly the observed turning point of the acute phase response was delayed by 3 days in WT mice (Fig. 4).

The time courses of virus-induced NREMS EEG SWA responses and duration of NREMS are different in both WT and AcPbKO mice (Fig. 3I and K). NREMS EEG SWA is often used as a measure of sleep intensity and sleep homeostasis. The separation of NREMS SWA from NREMS duration is exaggerated in the AcPbKO mice due to their large virus-induced reduction in NREMS EEG SWA beginning as early as PI Day 2. Such responses recapitulate the independent regulation of delta power from sleep duration (Davis et al., 2011). Regardless, AcPb seems to be involved in both sleep and EEG slow wave power.

It is not known the extent to which the AcPb-associated effects on sleep are localized to specific brain regions. IL1 β and its receptor increase with sleep loss in the hypothalamus, hippocampus, and cerebral cortex. Local application of IL1 to the somatosensory cortex enhances EEG NREMS SWA unilaterally and Fos immunoreactivity in associated cortical areas and hypothalamic sleep regulatory areas (Yasuda et al., 2005, 2007). Further, in rats and mice SD is followed by enhanced IL1 mRNA and AcPb mRNA expressions in the somatosensory cortex (Taishi et al., 1998, 2012; Zielinski et al., 2012). In rats, but not mice, SD enhances hypothalamic IL1 mRNA and injection of IL1 into the hypothalamic area enhances sleep (Alam et al., 2004) suggesting subcortical sites are also involved in mediating IL1-sleep effects. AcPb is also implicated in hippocampal synaptogenesis (Huang et al., 2011; Yoshida et al., 2012). Extended sleep deprivation compromises hippocampal neurogenesis and proliferation (Guzman-Marin et al., 2003; Garcia-Garcia et al., 2011). Recent evidence indicates that the type I IL1 receptor and glucocorticoids mitigate the detrimental effects of sleep loss on cell survival (Mueller et al., 2014). This protective role could result in part from AcPb, as AcPb facilitates neuronal survival following excitotoxicity (Gosselin et al., 2013). Thus the roles of IL1-signaling in brain extend beyond its classic

pro-inflammatory actions including neuronal plasticity and sleep regulation. Further, the contribution of AcPb to brain functions is illustrated by its ability to activate Src kinases independent of the canonical IL1 signaling pathway via NFkB (Huang et al., 2011) and its ability to act as a cell adhesion molecule (Yoshida et al., 2012).

Collectively these data provide strong evidence for an important role for AcPb in host defenses and sleep regulation. Our results add to the growing evidence that AcPb is integral to multiple diverse brain functions. Further, that a neuron-specific protein profoundly affects morbidity and mortality caused by a lung disease suggests alternative approaches to treatment and perhaps prevention of influenza virus-induced disease.

Acknowledgments

This work was supported by NIH grants NS025378 and HD036520 to J.M.K. and AG041287 to M.R.O. We thank Amgen (Thousand Oaks, CA) and Dirk Smith for providing the AcPb knock-out mice.

References

- Alam, M.N., McGinty, D., Bashir, T., Kumar, S., Imeri, L., Opp, M.R., Szymusiak, R., 2004. Interleukin-1 β modulates state-dependent discharge activity of preoptic area and basal forebrain neurons: role in sleep regulation. *Eur. J. Neurosci.* 20, 207–216.
- Besedovsky, L., Lange, T., Born, J., 2012. Sleep and immune function. *Pflügers Arch.* 463, 121–137.
- Cavadini, G., Petrzilka, S., Kohler, P., Jud, C., Tobler, I., Birchler, T., Fontana, A., 2007. TNF- α suppresses the expression of clock genes by interfering with E-box-mediated transcription. *Proc. Natl. Acad. Sci. U.S.A.* 104, 12843–12848.
- Conn, C.A., McClellan, J.L., Maassab, H.F., Smitka, C.W., Majde, J.A., Kluger, M.J., 1995. Cytokines and the acute phase response to influenza virus in mice. *Am. J. Physiol.* 268, R78–R84.
- Davis, C.J., Clinton, J.M., Jewett, K.A., Zielinski, M.R., Krueger, J.M., 2011. Delta wave power: an independent sleep phenotype or epiphenomenon? *J. Clin. Sleep Med.* 7, S16–S18.
- Fang, J., Sanborn, C.K., Renegar, K.B., Majde, J.A., Krueger, J.M., 1995. Influenza viral infections enhance sleep in mice. *Proc. Soc. Exp. Biol. Med.* 210, 242–252.
- Fang, J., Wang, Y., Krueger, J.M., 1998. The effects of interleukin-1 β on sleep are mediated by the type I receptor. *Am. J. Physiol.* 274, R655–R660.
- Franken, P., Chollet, D., Tafti, M., 2001. The homeostatic regulation of sleep need is under genetic control. *J. Neurosci.* 21, 2610–2621.
- García-García, F., De la Herrán-Arita, A.K., Juárez-Aguilar, E., Regalado-Santiago, C., Millán-Aldaco, D., Blanco-Centurión, C., Drucker-Colín, R., 2011. Growth hormone improves hippocampal adult cell survival and counteracts the inhibitory effect of prolonged sleep deprivation on cell proliferation. *Brain Res. Bull.* 84, 252–257.
- Gosselin, D., Bellavance, M.A., Rivest, S., 2013. IL-1RAcPb signaling regulates adaptive mechanisms in neurons that promote their long-term survival following excitotoxic insults. *Front. Cell. Neurosci.* 7, 1–12.
- Grimm, D., Staeheli, P., Hufbauer, M., Koerner, I., Martínez-Sobrido, L., Solórzano, A., García-Sastre, A., Haller, O., Kochs, G., 2007. Replication fitness determines high virulence of influenza A virus in mice carrying functional Mx1 resistance gene. *Proc. Natl. Acad. Sci. U.S.A.* 104, 6806–6811.
- Guzman-Marín, R., Suntsova, N., Stewart, D.R., Gong, H., Szymusiak, R., McGinty, D., 2003. Sleep deprivation reduces proliferation of cells in the dentate gyrus of the hippocampus in rats. *J. Physiol.* 549, 563–571.
- Huang, Y., Smith, D.E., Ibanez-Sandoval, O., Sims, J.E., Friedman, W.J., 2011. Neuron-specific effects of interleukin-1 β are mediated by a novel isoform of the IL-1 receptor accessory protein. *J. Neurosci.* 31, 18048–18059.
- Huber, R., Deboer, T., Tobler, I., 2000. Effects of sleep deprivation on sleep and sleep EEG in three mouse strains: empirical data and simulations. *Brain Res.* 857, 8–19.
- Imeri, L., Bianchi, S., Opp, M.R., 2006. Inhibition of caspase-1 in rat brain reduces spontaneous non-rapid eye movement sleep and non-rapid eye movement sleep enhancement induced by lipopolysaccharide. *Am. J. Physiol. Regul. Integr. Comp. Physiol.* 291, R197–R204.
- Imeri, L., Opp, M.R., 2009. How (and why) the immune system makes us sleep. *Nat. Rev. Neurosci.* 10, 199–210.
- Kuo, T.H., Williams, J.A., 2014. Acute sleep deprivation enhances post-infection sleep and promotes survival during bacterial infection in *Drosophila*. *Sleep* 37, 859–869.
- Krueger, J.M., 2008. The role of cytokines in sleep regulation. *Curr. Pharm. Des.* 14, 3408–3416.
- Krueger, J.M., Taishi, P., De, A., Davis, C., Winters, B.D., Clinton, J., Szentirmai, E., Zielinski, M.R., 2010. ATP and the purine type 2 X7 receptor affect sleep. *J. Appl. Physiol.* 109, 1318–1327.
- Leyva-Grado, V., Churchill, L., Wu, M., Williams, T.J., Taishi, P., Majde, J.A., Krueger, J.M., 2009. Influenza virus- and cytokine-immunoreactive cells in the murine olfactory and central autonomic nervous systems before and after illness onset. *J. Neuroimmunol.* 211, 73–83.
- Majde, J.A., Bohnet, S.G., Ellis, G.A., Churchill, L., Leyva-Grado, V., Wu, M., Szentirmai, E., Rehman, A., Krueger, J.M., 2007. Detection of mouse-adapted human influenza virus in the olfactory bulb of mice within hours after intranasal infection. *J. Neurovirol.* 13, 399–409.
- Majde, J.A., Kapas, L., Bohnet, S.G., De, A., Krueger, J.M., 2010. Attenuation of the influenza virus sickness behavior in mice deficient in Toll-like receptor 3. *Brain Behav. Immun.* 24, 306–315.
- Majde, J.A., Krueger, J.M., 2005. Links between the innate immune system and sleep. *J. Allergy Clin. Immunol.* 116, 1188–1198.
- Mueller, A.D., Parfyonov, M., Pavlovski, I., Marchant, E.G., Mistlberger, R.E., 2014. The inhibitory effect of sleep deprivation on cell proliferation in the hippocampus of adult mice is eliminated by corticosterone clamp combined with interleukin-1 receptor 1 knockout. *Brain Behav. Immun.* 35, 102–108.
- Opp, M.R., Obál Jr., F., Krueger, J.M., 1991. Interleukin-1 alters rat sleep: temporal and dose-related effects. *Am. J. Physiol.* 260, R52–R58.
- Smith, D.E., Lipsky, B.P., Russell, C., Ketchum, R.R., Kirchner, J., Hensley, K., Huang, Y., Friedman, W.J., Boissonneault, V., Plante, M.M., Rivest, S., Sims, J.E., 2009. A central nervous system-restricted isoform of the interleukin-1 receptor accessory protein modulates neuronal responses to interleukin-1. *Immunity* 30, 817–831.
- Taishi, P., Bredow, S., Guha-Thakurta, N., Obál Jr., F., Krueger, J.M., 1997. Diurnal variations of interleukin-1 β mRNA and β -actin mRNA in rat brain. *J. Neuroimmunol.* 75, 69–74.
- Taishi, P., Chen, Z., Obál Jr., F., Zhang, J., Hansen, M., Fang, J., Krueger, J.M., 1998. Sleep-associated changes in interleukin-1 β mRNA in the brain. *J. Interferon Cytokine Res.* 18, 793–798.
- Taishi, P., Davis, C.J., Bayomy, O., Zielinski, M.R., Liao, F., Clinton, J.M., Smith, D.E., Krueger, J.M., 2012. Brain-specific interleukin-1 receptor accessory protein in sleep regulation. *J. Appl. Physiol.* 112, 1015–1022.
- Tobler, I., Borbély, A.A., 1986. Sleep EEG in the rat as a function of prior waking. *Electroencephalogr. Clin. Neurophysiol.* 64, 74–76.
- Toth, L.A., Jhaveri, K., 2003. Sleep mechanisms in health and disease. *Comp. Med.* 53, 473–486.
- Toth, L.A., Rehg, J.E., Webster, R.G., 1995. Strain differences in sleep and other pathophysiological sequelae of influenza virus infection in naive and immunized mice. *J. Neuroimmunol.* 58, 89–99.
- Toth, L.A., Tolley, E.A., Krueger, J.M., 1993. Sleep as a prognostic indicator during infectious disease in rabbits. *Proc. Soc. Exp. Biol. Med.* 203, 179–192.
- Toth, L.A., Verhulst, S.J., 2003. Strain differences in sleep patterns of healthy and influenza-infected inbred mice. *Behav. Genet.* 33, 325–336.
- Vyazovskiy, V.V., Achermann, P., Tobler, I., 2007. Sleep homeostasis in the rat in the light and dark period. *Brain Res. Bull.* 74, 37–44.
- Wong, J.P., Saravolac, E.G., Clement, J.G., Nagata, L.P., 1997. Development of a murine hypothermia model for study of respiratory tract influenza virus infection. *Lab. Anim. Sci.* 47, 143–147.
- Yasuda, K., Churchill, L., Yasuda, T., Blindheim, K., Falter, M., Krueger, J.M., 2007. Unilateral cortical application of interleukin-1 β (IL1 β) induces asymmetry in fos IL1 β and nerve growth factor immunoreactivity: implications for sleep regulation. *Brain Res.* 1131, 44–59.
- Yasuda, T., Yoshida, H., García-García, F., Kay, D., Krueger, J.M., 2005. Interleukin-1 β has a role in cerebral cortical state-dependent electroencephalographic slow-wave activity. *Sleep* 28, 177–184.
- Yoshida, T., Shiroshima, T., Lee, S.-J., Yasumura, M., Uemura, T., Chen, X., Iwakura, Y., Mishina, M., 2012. Interleukin-1 receptor accessory protein organizes neuronal synaptogenesis as a cell adhesion molecule. *J. Neurosci.* 32, 2588–2600.
- Zielinski, M.R., Krueger, J.M., 2011. Sleep and innate immunity. *Front. Biosci. (Schol. Ed.)* 3, 632–642.
- Zielinski, M.R., Taishi, P., Clinton, J.M., Krueger, J.M., 2012. 5'-Ectonucleotidase-knockout mice lack non-REM sleep responses to sleep deprivation. *Eur. J. Neurosci.* 35, 1789–1798.